Industrial Crops & Products 185 (2022) 115142

Contents lists available at ScienceDirect

Industrial Crops & Products

journal homepage: www.elsevier.com/locate/indcrop

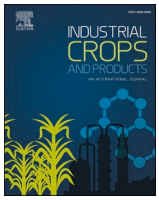

Sonoextraction of phenolic compounds and saponins from *Aesculus hippocastanum* seed kernels: Modeling and optimization

Maria Inês Dias [1], Carly Albiston [1], Mikel Añibarro-Ortega, Isabel C.F.R. Ferreira, José Pinela [*], Lillian Barros [*]

Centro de Investigação de Montanha (CIMO), Instituto Politécnico de Bragança, Campus de Santa Apolónia, Bragança 5300-253, Portugal

ARTICLE INFO

Keywords:
Horse chestnut seed extracts
Sonoextraction
Aescin saponins
Flavonol glycosides
Chromatographic analysis
Extraction optimization

ABSTRACT

The sonoextraction (SE) of aescin saponins and phenolic compounds from the inedible seed kernels of *Aesculus hippocastanum* was optimized using a central composite rotatable design coupled with response surface methodology, where the joint effects of ultrasonic power, sonication time, and ethanol proportion were investigated. Flavonol glycosides (≥90 % of the phenolic fraction), flavan-3-ols, phenolic acids, and aescin saponins were identified by HPLC-DAD-ESI/MS^n, and the quantitative data was fitted to a quadratic model to predict the optimal SE conditions. After validating the models, the significant effect of the three factors was confirmed. The extraction of flavonols was maximized to 48 ± 2 mg/g extract by SE at 105.9 W for 4.1 min in 83.9 % ethanol, while 19.9 min sonication at 100.9 W in 95.8 % ethanol favored the recovery of 3.8 ± 0.1 mg/g extract of aescin saponins. A process for simultaneous SE of both classes of phytochemicals was also established. Overall, these SE processes proved to be time-saving and selective for the *A. hippocastanum* seed active constituents, which are cognized for their wide range of bioactivities and applications in the pharmaceutical, cosmetic, and food industries.

1. Introduction

Horse chestnut (*Aesculus hippocastanum* L., Sapindaceae) is a widespread deciduous tree cultivated as an ornamental in urban areas across the Northern hemisphere. Its fruit is a green spiky capsule containing one to three nut-like seeds known as conkers (Zhang et al., 2014). The seeds and the bark of young branches of this three have been used in folk medicine and phytotherapy (Küçükkurt et al., 2010). In Europe, the seeds have long been used to treat venous disorders, particularly varicose veins and hemorrhoids, but also inflammatory ailments such as arthritis (Mitscher, 2007). Among the scientific community, horse chestnut seeds are mainly known for their steroidal glycosides. Aescin (or escin) is the main active component among the steroidal glycosides, and is responsible for most of the medicinal properties (Cheong et al., 2018; Jiang et al., 2011; Matsuda et al., 1997; Sirtori, 2001). However, other bioactive compounds such as flavonoids (mainly quercetin and kaempferol glycosides) have also been reported in the seeds (Čukanović et al., 2020), which are strong antioxidants and may interact with other compounds present in the extracts (Kochan et al., 2019).

Aescin is a complex mixture of triterpene saponin glycosides and exists in two forms (α and β) which can be distinguished by melting point, water solubility, and hemolytic potential (Aronson, 2016; Čukanović et al., 2020; Sirtori, 2001). β-Aescin, composed of aescin Ia and aescin Ib, appears to be more active than β-escin, which consist of isoescin Ia and isoescin Ib (Sirtori, 2001). The chemical structure of these four aescin constituents is shown in Fig. S1. The aglycon is derived from protoaescigenin, acylated by acetic acid at C-22 and by either angelic (A) or tiglic (T) acids at C-21, and has a trisaccharide group linked at C-3 (consisting of glucuronic acid and two glucose molecules) (EMA, 2020). Thus, due to the lipophilic sapogenin and water-soluble sugar chain, these have an amphiphilic nature and are surface active compounds (used as natural biosurfactants) (Liao et al., 2021). From a medicinal point of view, aescin is claimed to have clinical activity in chronic venous insufficiency (EMA, 2008). Investigations in animal models suggest that it has anti-inflammatory (Jiang et al., 2011; Zhao et al., 2018), anti-edematous (Zhao et al., 2018), and venotonic properties (Sirtori, 2001). Aescin also displays activity against various types of cancer, including lung adenocarcinoma, hepatocellular carcinoma,

* Corresponding authors.
E-mail addresses: jpinela@ipb.pt (J. Pinela), lillian@ipb.pt (L. Barros).
[1] The authors contributed equally to the work.

https://doi.org/10.1016/j.indcrop.2022.115142
Received 27 February 2022; Received in revised form 23 May 2022; Accepted 26 May 2022
Available online 3 June 2022

and leukemia cell models (Cheong et al., 2018; Zhao et al., 2022).

The bioactive potential of saponins and phenolic compounds have increased the exploitation of these natural compounds from plant materials, which has driven the emergence of novel extraction techniques with the aim of maximizing the process yield and extract quality in a sustainable way (Alara et al., 2021; Cheok et al., 2014). However, the extraction and isolation of phytoconstituents with such a great structural diversity can be very challenging as the extraction processes are affected by many factors related to the plant material, operation conditions, equipment, and solvent used (Cheok et al., 2014; Pinela et al., 2018). Ultrasound-assisted extraction or sonoextraction (SE) appears among the unconventional methods as a fast and low-cost technique that relies on the breakdown of the plant matrix by the implosion of acoustic cavitation bubbles in the solvent, which generates micromixing or turbulence and increases mass transfer (Chemat et al., 2017). However, SE processes are affected by equipment settings (*e.g.*, sonication time and power input) and sample/solution characteristics (*e.g.*, particle size, solid/liquid ratio, and solvent type), and classical one-factor-at-a-time optimization approaches are time-consuming and unable to assess interaction effects between factors, and may lead to false optimal conditions. Therefore, a statistical tool capable of identifying the terms that cause significant changes in the extraction process must be used, such as the response surface methodology (RSM). RSM describes the relationship between factors and response(s), allowing process modeling and optimization with a reduced number of runs. Moreover, the analytical methods used in the identification and quantification of compounds (to be used as response variables) should be the most accurate and reliable, as the colorimetric methods often referenced in Pharmacopoeias are not specific to individual compounds and may lead to possible overestimation (Chen et al., 2007).

To the best of the authors' knowledge, studies on the extraction optimization of horse chestnut seeds constituents are very scarce. Amiri et al. (2019) optimized the SE of fatty acids from the seeds and Vujic et al. (2013) optimized the extraction of triterpene glycosides (expressed as total aescin equivalents) from whole seeds, but using spectrophotometric data. Furthermore, Gagić et al. (2021) optimized the subcritical water extraction of different phytoconstituents and reported that aescin can be detected in peeled seed extracts, but not in the seed shell or in the bark or leaves of this tree. On the other hand, patented inventions for the production of aescin-rich extracts involve time-consuming extractions (up to 50 h) and some of them employ solvents such as propylene glycol that cannot be separated from the extract (Horvath, 1991; Kameyama and Fujimura, 2016; Kurt, 1965; Singh, 2006). Therefore, given the current need for innovative and more sustainable methodologies for the extraction of active phytochemicals from this plant matrix, this work was carried out to characterize the saponin and phenolic profiles of horse chestnut seed kernel extracts by HPLC-DAD-ESI/MS^n and to optimize the SE of the detected high value-added compounds using a five-level, three factor central composite rotatable design (CCRD, 5^3) coupled with RSM. It was also intended to investigate the SE conditions that simultaneously promote the recovery of both classes of bioactive compounds, in order to provide biorefineries with cost-effective processes.

2. Material and methods

2.1. Standards and plant material

The aescin standard (Alfa Aesar) was acquired from Enzymatic (Lisbon, Portugal) and the caffeic acid (Sigma-Aldrich), catechin, and quercetin-3-*O*-glucoside standards were acquired from Extrasynthèse (Genay, France) and had a purity level of at least 98 %.

Ripe horse chestnut fruits were collected in the orchards of the Polytechnic Institute of Bragança campus, Portugal. The seed kernel (cotyledons) was hand separated from the shell with a knife, freeze-dried, reduced to a fine powder until passing through a 20-mesh sieve, and stored under vacuum at −20 °C until use. For this study, the seed shell was removed because it does not contain aescin in its composition (at least in considerable amounts) (Gagić et al., 2021). In addition, the extracts will have a lighter color, thus representing an advantage when formulating pharmaceuticals, cosmetics, or other products.

2.2. Experimental design

In order to optimize the extraction of active phytoconstituents from horse chestnut seed kernels, a CCRD–RSM experiment was implemented considering the factors and ranges presented in Table 1. The entire power range (5–500 W) of the ultrasonic processor was included in the design. The same approach was followed for ethanol proportion (0–100 %, *v/v*). In turn, extraction times ranging from 1 to 45 min were selected based on previous studies (Caleja et al., 2017; Silva et al., 2021) and considering that SE has been described as a time-saving methodology. Even so, times of up to 45 min were considered to assess the impact of longer sonication on the target compounds. The 20-run design matrix was composed of 8 factorial points, 6 axial points, and 1 center point replicated 6 times. Randomization was used in the experiment.

2.3. Sonoextraction

One gram of sample was mixed with 50 mL of solvent (0–100 %) and sonicated at 5–500 W (20 kHz frequency) for 1–50 min according to the experimental design matrix in Table S1 (Supplementary material). A QSonica CL-334 (Newtown, Connecticut, USA) ultrasonic processor with titanium horn was used. The sample-to-solvent ratio was kept at 20 g/L, and a cold-water bath was used to prevent the temperature from rising above 25 ºC. After processing, the mixtures were centrifuged at 4000 × *g* for 10 min and the upper phase was recovered with a pipette; an aliquot was used to determine the recovered solids and the remaining portion was concentrated under reduced pressure and then freeze-dried to dryness.

2.4. Determination of extracted solids

A gravimetric method was followed to determine the recovered solids (or extraction yield, % *w/w*, weight of solids per weight of feed material). The extraction supernatants (4 mL) were placed into calcined crucibles and the solvent was evaporated at 105 °C for at least 24 h until constant weight was achieved (Silva et al., 2021).

2.5. HPLD-DAD-ESI/MS analysis of saponins and phenolic compounds

2.5.1. Chromatographic conditions

Each dry extract was dissolved in ethanol/water 20:80 (*v/v*) to a concentration of 10 mg/mL and filtered through a 0.22-μm syringe filters for injection in a Dionex Ultimate 3000 UPLC system (Thermo Scientific, San Jose, CA, USA) equipped with a diode array detector (DAD) and an electrospray ionization Linear Ion Trap LTQ XL mass spectrometer (ESI-MS) (Thermo Finnigan, San Jose, CA, USA). Separation was made on a Waters Spherisorb S3 ODS2- C18 (4.6 mm × 150 mm, 3 μm) column at 30 ºC. Elution was made with (A) 0.1 % HCOOH

Table 1
Code levels and actual experimental values of each experimental factor for SE processing.

Experimental factors	Symbols	Units	Coded variable levels				
			-1.68	-1	0	+1	+1.68
X_1: Time	*t*	min	1	10	23	36	45
X_2: Ultrasonic power	*P*	W	5	106	253	400	500
X_3: Ethanol proportion	*S*	%, *v/v*	0	20	50	80	100

and (B) CH_3CN. For phenolic compounds, the chromatographic analysis followed the specifications described by Bessada et al. (2016). For saponins, the conditions used were similar to those for phenolic compounds, but the following elution gradient was used: 20 % B (5 min), 20–25 % B (5 min), 25–35 % B (5 min), 35–60 % B (10 min), 60 % B (10 min), 60–25 % B (10 min), 25–20 % B (10 min), and column re-equilibration (10 min), using a flow rate of 0.5 mL/min. In both cases, analyses were made in negative ion mode. The DAD wavelengths were set at 260 nm for saponins and at 280 nm and 370 nm for phenolic compounds. Data were processed using Thermo Finnigan Xcalibur™ software.

2.5.2. Compound identification and quantification

Phenolic compounds were identified based on their chromatographic data (retention time and UV–vis and mass spectra) by comparison with available commercial standards and literature data. For quantification, seven-level calibration curves were constructed based on the UV–vis signal of the standards: caffeic acid ($y = 406{,}369 + 388{,}345x$, $r^2 = 0.9939$, limit of detection (LOD) = 0.78 μg/mL, limit of quantification (LOQ) = 1.97 μg/mL), catechin ($y = -23{,}200 + 84{,}950x$; $r^2 = 1$; LOD = 0.17 μg/mL; LOQ = 0.65 μg/mL), and quercetin-3-*O*-glucoside ($y = -160{,}173 + 34{,}843x$; $r^2 = 0.9998$; LOD = 0.21 μg/mL; LOQ = 0.71 μg/mL). For compounds with no available standard, quantification was done using the most similar standard calibration curve available.

Saponins were identified by comparing their chromatographic behavior with that of the standard compound and literature data. For quantification, a seven-level calibration curve (linearity range: 0.625–100 μg/mL) was constructed based on the UV signal of the aescin standard: escin Ia ($y = -27{,}844 + 92{,}371x$; $r^2 = 0.9995$; LOD = 1.42 μg/mL; LOQ = 4.31 μg/mL), escin Ib ($y = -46{,}743 + 87{,}703x$; $r^2 = 0.9999$; LOD = 0.78 μg/mL; LOQ = 2.35 μg/mL), isoescin Ia ($y = 11{,}457 + 120{,}190x$; $r^2 = 0.9999$; LOD = 0.66 μg/mL; LOQ = 1.99 μg/mL), and isoescin Ib ($y = -61{,}474 + 26{,}242x$; $r^2 = 0.9998$; LOD = 0.89 μg/mL; LOQ = 2.69 μg/mL). The results were expressed as mg equivalents (of its basic constituent or similar compound) per g of freeze-dried extract.

2.6. Extraction process modelling and statistical analysis

The following dependent (response) variables were considered for process optimization: Y_1 (solids, %, *w/w*), Y_2 (Σ phenolic acids, mg/g extract), Y_3 (Σ flavan-3-ols, mg/g extract), Y_4 (Σ flavonols, mg/g extract), Y_5 (Σ phenolic compounds, mg/g extract), Y_6 (β-aescin, mg/g extract), Y_7 (α-aescin, mg/g extract), and Y_8 (Σ saponins, mg/g extract). The RSM models were fitted using the following quadratic polynomial equation:

$$Y = b_0 + b_1X_1 + b_2X_2 + b_3X_3 + b_{11}X_1^2 + b_{22}X_2^2 + b_{33}X_3^2 + b_{12}X_1X_2 + b_{13}X_1X_3 + b_{23}X_2X_3 \quad (1)$$

where Y is to the response variable, X corresponds to the process factors, b_0 is the constant coefficient, b_1, b_2 and b_3 are linear term coefficients, b_{11}, b_{22} and b_{33} are quadratic term coefficients, and b_{12}, b_{13} and b_{23} are interaction term coefficients.

Models' fitting procedures, coefficient estimates, and statistical analyses were performed using Design-Expert software, which was also used to generate the 2D and 3D plots. ANOVA was used to assess the statistical significance ($p < 0.05$) of the models and of all their parametric terms, as well as the lack-of-fit (Rocha et al., 2020). The coefficients R^2 and adjusted (*Adj*) R^2, the adequate precision (a signal-to-noise ratio), and the coefficient of variation or relative standard deviation were assessed for statistical verification of the polynomial models.

3. Results and discussion

3.1. Phytochemical profile

The phytochemical profile of the horse chestnut seed kernel extracts was characterized by HPLC-DAD-ESI/MS^n and the retention time, λ_{max} in the UV–vis region, pseudomolecular ion, and main fragment ions used in the identification of phenolic compounds are shown Table 2. A representative chromatogram of the phenolic profile is shown in Fig. 1A (A1 was recorded at 280 nm and A2 at 370 nm). Fifteen phenolic compounds were identified in the seed sample, including three phenolic acids (caffeic acid derivatives), two flavan-3-ols (catechin derivatives), and ten flavonols (*O*-glycosylated quercetin, kaempferol, and isorhamnetin derivatives). The phenolic compounds identified in these samples coincided with those previously described by Dridi (2018), except for compound **12** ($[M-H]^-$ at *m/z* 609, quercetin-3-*O*-rutinoside) whose identification was performed in comparison to the retention time and λ_{max} with the available commercial standard. Additionally, the chromatographic data of each peak was also compared with the data provided by the authors referenced in Table 2.

The chromatographic analysis allowed for the identification of the four main aescin saponins in the horse chestnut seed kernel extracts, namely aescin Ia and aescin Ib (β-aescin) and isoaescin Ia and isoaescin Ib (α-aescin), which have also been detected in the seeds of the congeneric *Aesculus chinensis* Bunge (Chen et al., 2007). As observed in the representative chromatogram in Fig. 1B (B1 for kernel extracts and B2 for aescin standard), β-aescin predominated over α-aescin, which agrees with previous reports (Abudayeh et al., 2015). In addition, β-aescin has been described as the main active component of horse chestnut seeds (Sirtori, 2001). The structural differences among the detected aescin saponins are illustrated in Fig. S1 (Supplementary material).

In order to provide quantitative data for each compound detected in the kernel extracts, the results from the six replicates of the center point of the design were selected and the mean relative percentage was calculated. As shown in Fig. 2, about 25.3 % of the phenolic fraction consisted of kaempferol-*O*-pentosyl-*O*-hexosyl-*O*-hexoside (compound **10**), followed by 23 % of isorhamnetin-*O*-pentosyl-*O*-dihexoside (compounds **7** and **11**), 17 % of quercetin-*O*-dihexosyl-pentoside (compounds **6** and **8**), and 12.1 % of quercetin-3-*O*-xylosyl-glucoside-3′-*O*-(6-*O*-nicotinoyl)-glucoside (compound **9**). The prevalence of these compounds reinforces the bioactivity of the extracts, since flavonols are a class of dietary flavonoids with strong antioxidant properties (Xiao et al., 2021). On the other hand, escin Ib (compound **17**) and isoescin Ib (compound **19**) predominated among the saponosides, with relative percentages of 36.9 % and 32.4 %, respectively. Furthermore, β-aescin prevailed over α-aescin with 58.3 % *versus* 41.7 %, which was not always verified when considering the factorial and axial points of the design matrix.

3.2. Quantitative experimental data for SE optimization

For optimization of the SE processes, the extracted solids (%, *w/w*) and the total contents (mg/g extract) of phenolic acids, flavan-3-ols, flavonols, phenolic compounds, β-aescin, α-aescin, and aescin saponins obtained with the 20 runs of the experimental design matrix were used as response variables (Table 3). For each group of compounds, the values resulted from the sum of the contents of the individual compounds quantified in each extract.

The solids extracted from the horse chestnut seed kernel ranged from 8.67 % (*w/w*) to 47.51 % (*w/w*) (Table 3). The highest solid extraction was achieved in the 4th run, which combined a medium-high extraction time and ultrasonic power (40 min and 400 W, respectively; +1 level), and a medium-low ethanol concentration (20 %, *v/v*; −1 level). In turn, the 14th run resulted in the lowest solid extraction and combined a medium extraction time and ultrasonic power (26 min and 253 W, respectively; 0 level) and 100 % ethanol (+1.68 level).

As observed in Table 3, the levels of extracted phenolic compounds

Table 2
Phenolic compounds identified in the horse chestnut seed kernel extract. The retention time (Rt), maximum absorption wavelengths in the UV–vis region (λ_{max}), and pseudomolecular and MS^2 fragment ions are presented.

Peak	Rt (min)	λ_{max} (nm)	$[M-H]^-$ (*m/z*)	MS^2 (*m/z*)	Tentative identification	Identification/ reference
Phenolic compounds						
1[a]	4.71	324	341	179(100), 161(15)	Caffeic acid hexoside	UV–vis/MS
2[b]	5.58	283	1153	865(68), 575(40), 577(22), 713(20), 287(10), 425 (5), 407(5), 289(5), 695(2)	β-Type (epi)catechin tetramer	Barros et al. (2015)
3[b]	6.71	283	863	695(100), 739(92), 577(69), 713(59), 575(49), 425(14), 287(12), 407(10), 289(6)	β-Type (epi)catechin trimer	Melgar et al. (2017)
4[a]	7.72	296	630	468(100), 306(100), 112(100), 289(54), 174(20), 262(1)	Tris-caffeoyl-spermidine	Dridi (2018)
5[a]	9.26	270	468	306(100), 262(33), 174(12), 130(2), 289(2)	Dicaffeoyl-spermidine	Dridi (2018)
6[c]	11.91	350	757	595(100), 301 (100), 463(29)	Quercetin-*O*-dihexosyl-pentoside	Kapusta et al. (2007)
7[c]	13.32	352	771	639(100), 315(100)	Isorhamnetin-*O*-pentosyl-*O*-dihexoside	Lin et al. (2008)
8[c]	14.26	350	757	595(100), 301 (100), 463(29)	Quercetin-*O*-dihexosyl-pentoside	Kapusta et al. (2007)
9[c]	16.01	353	862	595(100), 301(54), 445(47), 463(32), 475(18)	Quercetin-3-*O*-xylosyl-glucoside-3′-*O*-(6-*O*-nicotinoyl)-glucoside	Kapusta et al. (2007)
10[c]	17.06	349	741	609(100), 285(77), 447(46)	Kaempferol-*O*-pentosyl-*O*-hexosyl-*O*-hexoside	Kapusta et al. (2007)
11[c]	18.09	352	771	639(100), 315(100)	Isorhamnetin-*O*-pentosyl-*O*-dihexoside	Lin et al. (2008)
12[c]	19.11	343	609	301(100)	Quercetin-3-*O*-rutinoside	UV–vis/MS
13[c]	19.87	353	979	595(100), 301(54), 445(47), 463(32), 475(18)	Quercetin-3-*O*-xylosyl-glucoside-3′-*O*-(6-*O*-indolin-2-one-3-hydroxy-3-acetyl)-glucoside	Hübner et al. (1999)
14[c]	20.19	353	979	595(100), 301(54), 445(47), 463(32), 475(18)	Quercetin-3-*O*-xylosyl-glucoside-3′-*O*-(6-*O*-indolin-2-one-3-hydroxy-3-acetyl)-glucoside	Hübner et al. (1999)
15[c]	24.23	353	921	595(100), 301(54), 445(47), 463(32), 475(18)	Quercetin-3-*O*-rhamnosyl-glucosyl-glucuronide	Hübner et al. (1999)
Aescin saponins						
16[d]	29.26	220	–	–	Aescin Ia	UV
17[e]	29.52	221	–	–	Aescin Ib	UV
18[f]	30.38	223	–	–	Isoaescin Ia	UV
19[g]	31.68	221	–	–	Isoaescin Ib	UV

[a] Caffeic acid.
[b] Catechin.
[c] Quercetin-3-*O*-glucoside.
[d] Escin Ia.
[e] Escin Ib.
[f] Isoescin Ia.
[g] Isoescin Ib (standards used in the quantification; see subsection 2.5.2.).

varied with the 20 runs of the experimental design. These compounds ranged from 16.45 mg/g extract to 44.69 mg/g extract. Within this group of compounds, the flavonols were the most prominent, comprising more than 90 % of the phenolic compounds quantified in the extracts, while flavan-3-ols represent 2.9–7.1 %, and phenolic acids only 0.4–1.8 % of the phenolic fraction. The 14th run (which yielded the lowest weight of extracted solids and used 100 % ethanol) was the run with the highest content of phenolic compounds (44.46 mg/g extract), including flavonols (96.4 % of the phenolic fraction). On the other hand, the 4th run (which had the highest solid extraction and used 20 % ethanol) resulted in a low phenolic content of 18.81 mg/g extract, while the 12th run had the lowest phenolic content, of only 16.45 mg/g extract, as it used the highest ultrasonic power setting (500 W; +1.68 level), with a medium extraction time and ethanol concentration (26 min and 50 % ethanol, respectively; 0 level). These opposing extraction trends for solids and phenolic compounds evidence a possible selectivity for phenolic compounds as a function of the applied SE conditions.

In the case of flavan-3-ols and phenolic acids, these ranged from 0.762 to 1.560 mg/g extract and from 0.080 to 0.373 mg/g extract, respectively (Table 3). In both cases, the highest levels were obtained with the 8th run, followed by the 14th run. The conditions associated with the 3rd and 4th run were the least suitable for the extraction of these secondary metabolites, probably due to the use of medium-low ethanol concentrations (−1 level).

Regarding saponins, the total contents ranged from 0.818 to 3.392 mg/g extract (Table 3). The 14th run that promoted the recovery of phenolic compounds also led to high concentrations of aescin saponins, more specifically of β-aescin (2.26 mg/g extract). In turn, the highest levels of α-aescin (2.43 mg/g extract) were obtained with the 1st run of the experimental design. It was interesting to note that the proportion of the two forms (α and β) in the total aescin content varied greatly with the different SE conditions applied (α-aescin ranged from 27.4 % to 85.9 % and β-aescin from 14.1 % to 72.6 %). This remarkable variation in proportion can be explained manly by the solvent composition, since α-aescin is water-soluble while β-aescin is relatively water-insoluble (Aronson, 2016).

3.3. Models fitting and statistical verification

Polynomial models are useful to estimate and predict the shape of response values over a range of input values. Therefore, the experimental data in Table 3 was fitted to the quadratic Eq. (1) using Design-Expert and the generated polynomial models, expressed in coded values, are presented in Eqs. (A.1)–(A.8) in Supplementary material. Only the significant coefficients ($p < 0.05$) were considered in the fitting process. The results of the regression analysis and the statistical criteria used in the validation of these model equations are presented in Table 3.

In the theoretical models constructed for each response variable, the coefficients of the terms *t*, *P*, and *S* translate the effect of the factors time, ultrasonic power, and ethanol concentration, respectively, as well as their linear, quadratic, and interactive effects, when they exist. Since the expected responses are denoted by the coefficient values, the higher these values (regardless of the sign), the more significant the weight of the respective factor will be. For interactions, synergistic effects between factors are represented by a positive sign, while an antagonism is translated by a negative sign (Rocha et al., 2020). In Supplementary Eqs. (A.1)–(A.8) (A.1)–(A.8), the intercept corresponds to the expected mean value of the response variable (*Y*) when all factors are equal to zero ($X = 0$), *i.e.*, the predicted average response at the center point. Thus,

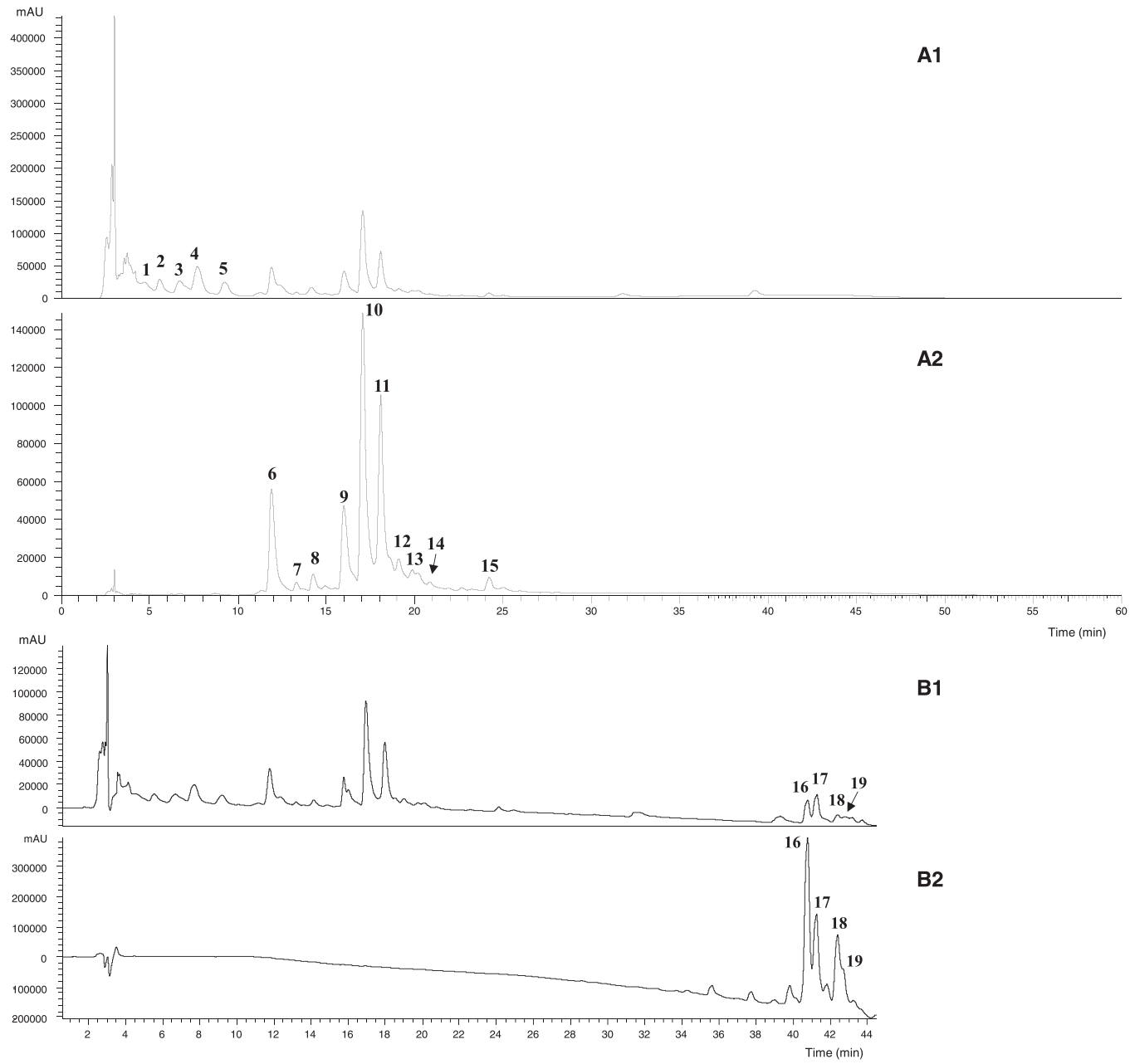

Fig. 1. Representative chromatograms of the phenolic profile of horse chestnut kernel extracts, registered at 280 nm (A1) and 370 nm (A2), and of the saponin profile of kernel extracts (B1) and aescin standard (B2), registered at 260 nm. Compounds identification is described in Table 2.

the intercept values in Table 4 also show which classes of compounds are most abundant in the sample under study.

As shown in Table 4 for the modelling statistics, the polynomial model Eqs. (A.1)–(A.8) presented significant F-values ($p < 0.05$) and a non-significant lack-of-fit ($p > 0.05$), which indicated that the constructed models adequately describe the effects of the factors on the target responses (Iberahim et al., 2019). In all cases, the coefficients R^2 and *Adj* R^2 were higher than 0.923 and 0.909, respectively, indicating that the variability of each response is explained by the factors involved in the SE process. In addition, adequate precision, which is a measure of the signal-to-noise ratio, had values greater than 23 (ratios > 4 indicate adequate model discrimination). The high degree of accuracy and reliability was also demonstrated by the low values of the coefficient of variation or relative standard deviation, which is a measure of the residual variation of the data relative to the size of the mean (Table 4). Thus, the developed theoretical models were statistically reliable for navigating the design space and subsequent optimization of the SE of solids, phenolic compounds, and saponins from the seed kernel of horse chestnut.

Important information about the individual and combined effects of the experimental factors on the SE of target compounds from the horse chestnut seed kernel can be gleaned from the model equations. As observed in Supplementary Eq.(A.1), the extraction of solids was significantly ($p < 0.05$) affected by the three factors involved in the process, mainly by the ethanol proportion, which caused marked negative linear and quadratic effects. The ultrasonic power came in second with positive linear effects and then processing time. The interaction of the solvent with the other two process factors was also observed (Table 4). This result supports RSM as an optimization method, since one-factor-at-a-time approaches fail to evaluate interaction effects. The extraction trends of phenolic compounds from the kernel are reflected in Supplementary Eqs. (A.2)–(A.5). Since flavonols constituted

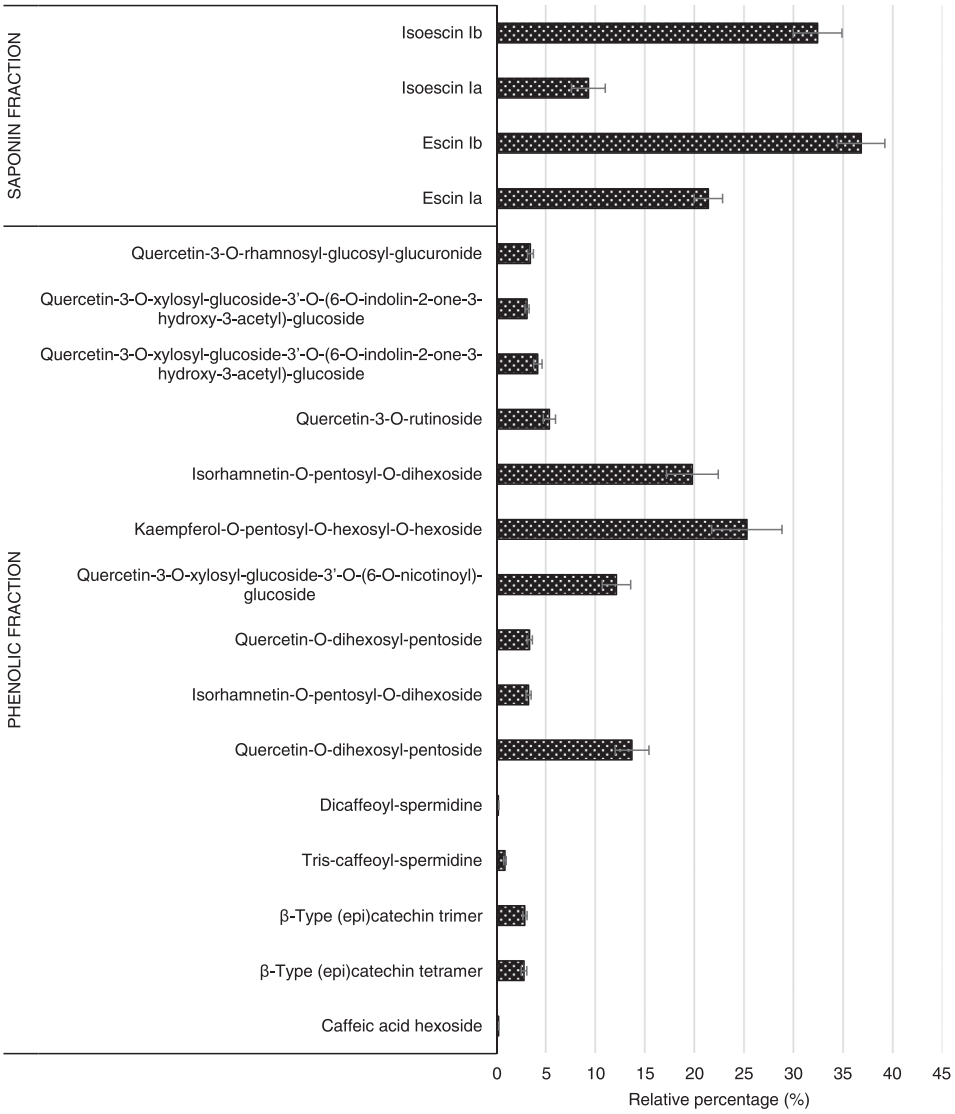

Fig. 2. Relative mean composition in phenolic compounds and aescin saponins of the phenolic and saponin fractions, respective, of the seed kernel extracts obtained with the 6 replicates of the center point of the experimental design in Table 3.

most of the phenolic fraction, Eqs. (A.4 and A.5, for flavonols and phenolic compounds, respectively) presented a comparable complexity, in which the weight of the coefficients was comparable. The solvent was once again the most impacting factor, noted for the positive linear effects, *i.e.*, the greater the ethanol proportion, the greater is the extraction of these compounds. This factor together with the extraction time also had noticeable positive quadratic effects (Table 4). In turn, Supplementary Eq. (A.2) and Eq. (A.3) referring to phenolic acids and flavan-3-ols, respectively, were only assembled by the linear and interaction terms of the solvent and power factors. For aescin saponins, Supplementary Eq. (A.6)–(A.8) brought together more terms than those for phenolic compounds, thus translating a more complex SE process. Actually, Eq. (A.8) gathered all the terms of the quadratic model Eq. (1) used to fit the theoretical models.

3.4. Effect of the experimental factors and optimal SE conditions

Three-dimensional response surface plots were constructed to visually show the effect of the three experimental factors on the extraction of solids, phenolic acids, flavan-3-ols, flavonols, phenolic compounds, β-aescin, α-aescin, and aescin saponins from the seed kernel of horse chestnut (Figs. 3 and 4). The grid surfaces were built using the theoretical values predicted with the quadratic polynomial Eq. (1). In each plot, the omitted factor was fixed at its individual optimal value presented in Table 5. For numerical optimization, to determine the experimental conditions that meet the desired objective (yield maximization), the factors *t*, *P* and *S* were set within the experimental domain (Table 1), while each target response was "maximized".

As illustrated in Fig. 3, solids recovery was promoted by the application of high ultrasonic power during long processing times, using low ethanol proportions. These extraction trends are also depicted in the 2D plots in Fig. 5 and are in agreement with those described by other authors for SE of solids from *Cytinus hypocistis* (L.) L. (Silva et al., 2021) and kiwi peel (Giordano et al., 2021). It is likely that the combination of these factors at a more intense level increased cell disruption and particle breakdown (sonoporation) promoted by the strong shear force caused in the medium by acoustic cavitation (Meullemiestre et al., 2016), with a consequent greater solvent penetration and release of extractable solids (including water-soluble carbohydrates). According to the model-predicted optimal SE conditions presented in Table 5, 52 ± 2 % (*w/w*) of solids can be achieved by sample sonication at 500 W for 36.7 min, using 27.6 % ethanol. Higher yields, around 85 % (*w/w*), were obtained by Gagić et al. (2021) by subcritical water extraction at 150 °C for 15 min or at 200 °C for 5 min. Despite this, the authors observed that

Table 3
Experimental responses of extracted solids and different phytochemicals obtained by SE from horse chestnut seed kernel.

Runs	Experimental domain			Experimental responses[a]							
	X_1: t (min)	X_2: P (W)	X_3: S (%)	Y_1: Solids	Y_2: Phenolic acids	Y_3: Flavan-3-ols	Y_4: Flavonols	Y_5: Phenolics	Y_6: β-Aescin	Y_7: α-Aescin	Y_8: Aescin saponins
1	11 (−1)	106 (−1)	20 (−1)	20.43	0.314	1.359	25.89	27.56	0.919	2.430	3.349
2	40 (+1)	106 (−1)	20 (−1)	32.54	0.335	1.336	17.25	18.92	0.634	0.189	0.823
3	11 (−1)	400 (+1)	20 (−1)	39.02	0.080	0.762	19.73	20.57	0.822	0.663	1.485
4	40 (+1)	400 (+1)	20 (−1)	47.51	0.084	0.803	17.92	18.81	0.702	0.115	0.818
5	11 (−1)	106 (−1)	80 (+1)	12.52	0.275	1.250	40.14	41.67	2.165	1.227	3.392
6	40 (+1)	106 (−1)	80 (+1)	13.30	0.270	1.239	37.18	38.69	1.930	1.070	3.000
7	11 (−1)	400 (+1)	80 (+1)	18.79	0.327	1.477	38.30	40.10	1.630	0.433	2.063
8	40 (+1)	400 (+1)	80 (+1)	22.75	0.373	1.560	33.55	35.48	1.560	1.570	3.130
9	1 (−1.68)	253 (0)	50 (0)	21.99	0.258	1.210	34.60	36.07	1.674	1.460	3.134
10	50 (+1.68)	253 (0)	50 (0)	33.31	0.217	1.200	26.12	27.54	1.200	0.587	1.787
11	26 (0)	5 (−1.68)	50 (0)	23.24	0.305	1.211	26.78	28.30	1.195	1.390	2.585
12	26 (0)	500 (+1.68)	50 (0)	42.99	0.201	1.070	15.18	16.45	0.562	0.487	1.049
13	26 (0)	253 (0)	0 (−1.68)	29.16	0.137	0.852	17.47	18.46	0.576	0.943	1.519
14	26 (0)	253 (0)	100 (+1.68)	8.67	0.350	1.480	42.86	44.69	2.260	1.123	3.383
15	26 (0)	253 (0)	50 (0)	35.92	0.212	1.041	20.31	21.56	0.935	0.693	1.628
16	26 (0)	253 (0)	50 (0)	34.15	0.220	1.163	16.62	18.00	0.704	0.989	1.692
17	26 (0)	253 (0)	50 (0)	29.88	0.251	1.200	24.64	26.09	0.704	0.486	1.190
18	26 (0)	253 (0)	50 (0)	33.10	0.300	1.294	20.45	22.04	0.836	0.600	1.436
19	26 (0)	253 (0)	50 (0)	35.18	0.219	1.215	20.70	22.13	0.865	0.582	1.447
20	26 (0)	253 (0)	50 (0)	33.66	0.232	1.278	21.03	22.53	0.984	0.716	1.700

[a] The mean values for extracted solids (%, *w/w*) and the different phytochemicals (mg/g extract) resulted from three determinations.

Table 4
Model coefficients estimated with the quadratic polynomial Eq. (1) and statistical data of the models' fitting procedure.

Coefficients[a]		Y_1: Solids	Y_2: Phenolic acids	Y_3: Flavan-3-ols	Y_4: Flavonols	Y_5: Phenolics	Y_6: β-Aescin	Y_7: α-Aescin	Y_8: Aescin saponins
Intercept	b_0	33.5 ± 0.8	0.248 ± 0.006	1.20 ± 0.01	20.9 ± 0.8	22.3 ± 0.8	0.85 ± 0.03	0.68 ± 0.06	1.52 ± 0.07
Linear effect	b_1	3.3 ± 0.6	ns	ns	-2.4 ± 0.6	-2.4 ± 0.6	-0.11 ± 0.03	-0.24 ± 0.04	-0.35 ± 0.05
	b_2	6.0 ± 0.6	-0.037 ± 0.007	-0.06 ± 0.02	-2.2 ± 0.6	-2.3 ± 0.6	-0.15 ± 0.03	-0.27 ± 0.04	-0.41 ± 0.05
	b_3	-7.8 ± 0.6	0.058 ± 0.007	0.17 ± 0.02	8.1 ± 0.6	8.4 ± 0.6	0.52 ± 0.03	0.09 ± 0.04	0.60 ± 0.05
Quadratic effect	b_{11}	-2.2 ± 0.6	ns	ns	3.7 ± 0.6	3.7 ± 0.6	0.22 ± 0.03	0.11 ± 0.04	0.33 ± 0.05
	b_{22}	ns	ns	ns	ns	ns	ns	ns	0.10 ± 0.05
	b_{33}	-5.2 ± 0.6	ns	ns	3.6 ± 0.6	3.6 ± 0.6	0.21 ± 0.03	0.11 ± 0.04	0.32 ± 0.05
Interaction effect	b_{12}	ns	ns	ns	ns	ns	ns	0.37 ± 0.05	0.41 ± 0.05
	b_{13}	-2.0 ± 0.8	ns	ns	ns	ns	ns	0.47 ± 0.05	0.48 ± 0.05
	b_{23}	-2.2 ± 0.6	0.080 ± 0.009	0.21 ± 0.02	ns	ns	0.21 ± 0.03	0.19 ± 0.05	0.32 ± 0.05
Modeling statistics									
Model F-value		58.79	64.40	64.29	55.82	57.17	98.57	30.92	60.90
Lack-of-Fit		0.4555	0.9300	0.9691	0.7321	0.7556	0.8364	0.8927	0.7133
R^2		0.9717	0.9235	0.9234	0.9522	0.95633	0.9785	0.9653	0.9779
Adj R^2		0.9551	0.9092	0.9090	0.9352	0.9366	0.9686	0.9341	0.9619
Adequate precision		30.13	25.21	26.43	23.91	24.27	30.72	23.70	23.22
Coefficient of variation (%)		7.74	9.88	5.35	8.66	8.23	8.35	15.76	8.66

[a] The parametric subscripts 1, 2, and 3 stand for time, power, and ethanol proportion, respectively.

at 150ºC, the amount of aescin decreases with increasing extraction time, while it was completely degraded after 5 min at 200ºC.

As shown in Figs. 4 and 5, the extraction of flavonols and phenolic compounds followed a trend opposite to that discussed for solids. The ethanol proportion was also the most impacting factor, but higher proportions were more appropriate for these seed constituents. The effect of time and power was negative, according to the sign of the parametric values in Table 4, as these intensifying factors may have led to the degradation of the compounds by cavitation phenomena. Thus, since short SE at low power with high ethanol proportions favor the extraction of flavonols and not solids, it will be possible to obtain seed extracts with greater purity in these bioactive compounds thanks to the selectivity of the process, thus representing an operational and cost-saving advantage. As shown in Table 5, these optimal SE conditions can yield 48 ± 2 mg/g extract of flavonols and 50 ± 2 mg/g extract of phenolic compounds, while the solids yield is around 13.6 % (*w/w*). Therefore, it is possible to recover about 6.53 mg of flavonols and 6.80 mg of phenolic compounds from 1 g of plant material. This result highlights the seed kernel as a good source of flavonol antioxidants with potential to be used in nutraceuticals and functional foods, but also in therapeutic products.

For the other two groups of phenolic compounds, those of flavan-3-ols and phenolic acids, the extractions were largely unaffected by time (Figs. 4 and 5), while the solvent and ultrasonic power factors interacted positively with each other (Table 4). Thus, as observed in the corresponding 3D plots in Fig. 4, although the maximum response was promoted by the application of high powers (311–314 W) with high ethanol proportions close to or equal to 100 % (Table 5), the use of opposite conditions also provided a slight increase in extraction.

The effects of the process factors on the extraction of aescin saponins are also shown in the 3D and 2D plots in Figs. 3 and 5, respectively. As observed for all groups of phenolic compounds, high ethanol proportions promoted the extraction of β-aescin and aescin saponins, whereas α-aescin was better recovered with low proportions. As discussed above, this result can be justified by the water solubility of α-aescin (Aronson, 2016). For both forms of aescin, lower processing times and ultrasonic powers were preferable. As shown in Table 5, 2.47

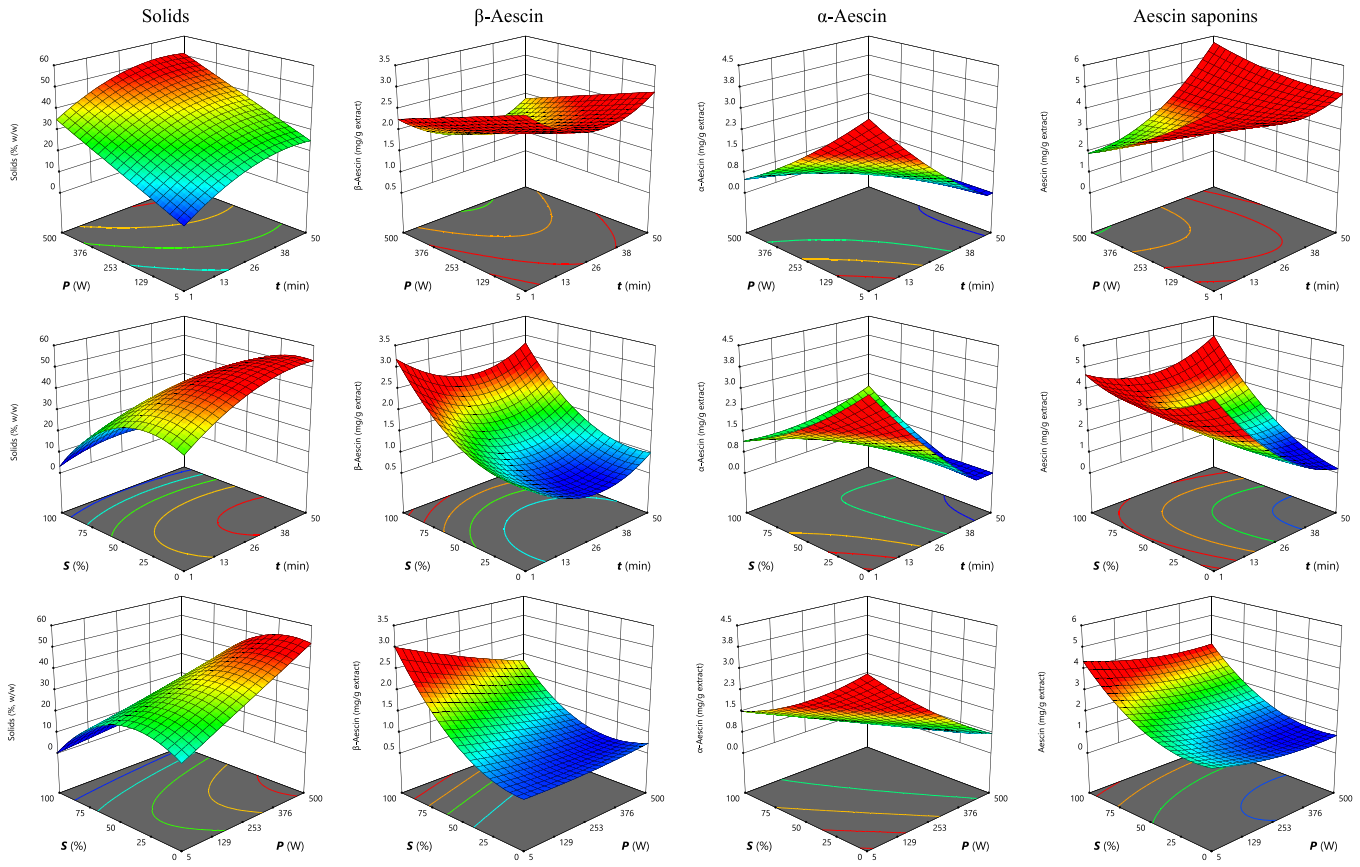

Fig. 3. Three-dimensional plots for the joint effects of the factors *t* (time), *P* (power) and *S* (ethanol proportion) on the sonoextraction of solids (Y_1) and aescin saponins (Y_6–Y_8) from horse chestnut seed kernel. In each plot, the omitted factor was fixed at its individual optimum in Table 5.

± 0.07 mg/g extract of β-aescin can be obtained from horse chestnut seed kernel when extracting at 212.7 W for 2.9 min using 83.7 % ethanol, and 2.5 ± 0.01 mg/g extract of α-aescin when sonicating the sample at 108.9 W for 8.3 min in 26.2 % ethanol. A total of 3.8 mg/g extract of aescin saponins can be obtained from this inedible seed, with about 13.5 % (*w*/*w*) of solids, corresponding to approximately 0.51 mg/g of plant material. However, the optimal SE conditions defined for aescin saponins require 19.9 min processing in 95.8 % ethanol.

In a previous work, Vujic et al. (2013) optimized the extraction of total triterpene glycosides from horse chestnut seeds using a DIG-MAZ extraction equipment and 67 % ethanol. A two-level full factorial design combined with a Derringer's desirability function was implemented considering the processing time (3–6 h), temperature (25–45ºC), and flow rate (125–345 mL/min), but quantitative data was obtained using a non-specific method towards individual aescin. The higher yield was achieved by processing at 45ºC for 3 h, at a flow rate of 125 mL/min, thus being a much more time-consuming process than that developed in the present study. Moreover, in addition to the possible overestimation associated with the spectrophotometric method, the optimal processing values were positioned at the extremes of the experimental design, which may indicate the need to expand the range of values of the experimental factors.

Patented methods for production of aescin-rich extracts from horse chestnut are also available for industrial exploitation. Kurt (1965) developed a process for obtaining propylene glycol extracts suitable for the treatment of skin defects and diseases. It consisted of macerating the peeled seed powder with propylene glycol at room temperature for 3 h, with occasional stirring. Later, Horvath (1991) described a method in which crushed seeds are extracted by stirring or circulating water for 3–50 h (variable depending on the temperature and degree of shredding of the sample). In turn, Kameyama and Fujimura (2016) patented the obtention of seed extracts from Hippocastanaceae plants, such as *A. hippocastanum*, *A.* chinensis, or *A. turbinata*, which were claimed to contain aescin and anti-inflammatory and astringent effects. For this, the crushed material was mixed with 50 % ethanol, stirred for 24 h at 50 °C, and the residue obtained after filtration was reextracted under the same conditions with an additional volume of the same hydroalcoholic solvent. A process for obtaining β-aescin from *A. indica* was also developed by Singh (2006), which involved the cold extraction of the plant material in a percolator with a hydroalcoholic mixture (methanol/ethanol and water, 1:1–8:2), repeated 6–8 times. In general, all these processes take much longer than those developed in this study for aescin saponins (Table 5), which therefore may represent higher processing costs.

Furthermore, although water was used in some of these methods, the trends in Fig. 5 show that this is not the most suitable solvent for β-aescin. In this work, the use of a new methodological process intensified by ultrasound and optimized by RSM allowed to maximize yields and understand how the target compounds are affected by the applied SE conditions. Thus, these methods represent a technological advance and could be exploited by biorefineries to provide bioactive extracts and ingredients in a more sustainable way.

3.5. Global optimal SE condition for phenolic compounds and aescin saponins

After determining the SE conditions that maximize each response to its maximum value, a second optimization step was performed to simultaneously maximize the extraction of phenolic compounds (Y_5) and aescin saponins (Y_8). As presented in Table 5, 48 ± 2 mg of phenolic compounds and 3.8 ± 0.1 mg of aescin saponins can be obtained per gram of extract when sonicating the seed kernel in 98.4 % ethanol at

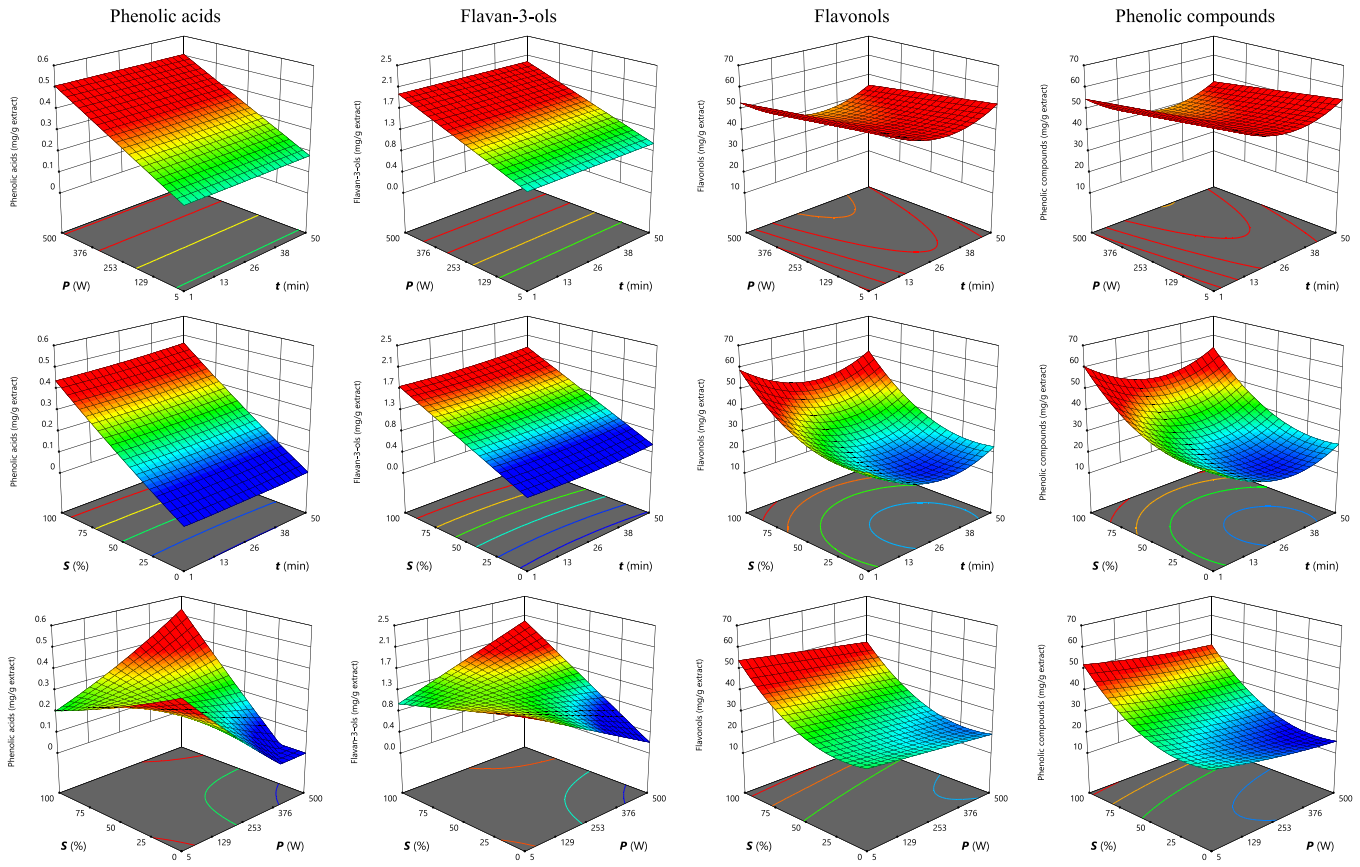

Fig. 4. Three-dimensional plots for the joint effects of the factors *t* (time), *P* (power) and *S* (ethanol proportion) on phenolic compounds (Y_2–Y_5) recovered from horse chestnut seed kernel. In each plot, the omitted factor was fixed at its individual optimum in Table 5.

Table 5
Optimal processing conditions that maximize the SE of phenolic compounds and saponins from the horse chestnut seed kernel and model-predicted optimal response values.

Responses	Optimal processing conditions			Response optimum
	X_1: *t* (min)	X_2: *P* (W)	X_3: *S* (%, *v*/*v*)	
	Individual conditions for each response variable			
Y_1: Solids	36.7	500	27.6	52 ± 2 % (*w*/*w*)
Y_2: Phenolic acids	11.8	310.9	99.7	0.38 ± 0.01 mg/g extract
Y_3: Flavan-3-ols	7.5	314.4	99.0	1.60 ± 0.04 mg/g extract
Y_4: Flavonols	4.1	105.9	83.9	48 ± 2 mg/g extract
Y_5: Phenolic compounds	7.6	126.7	91.1	50 ± 2 mg/g extract
Y_6: β-Aescin	2.9	212.7	83.7	2.47 ± 0.07 mg/g extract
Y_7: α-Aescin	8.3	108.9	26.2	2.5 ± 0.1 mg/g extract
Y_8: Aescin saponins	19.9	100.9	95.8	3.8 ± 0.1 mg/g extract
	Global conditions for all compounds			
Y_5: Phenolic compounds	22.0	125.1	98.4	48 ± 2 mg/g extract
Y_8: Aescin saponins				3.8 ± 0.1 mg/g extract

125.1 W for 22.0 min. Thus, it will be possible to obtain high levels of both groups of active constituents with a loss of only 3 % of phenolics and 0.3 % saponins in relation to the levels achieved with the individual processing conditions.

4. Conclusions

The phenolic fraction of the seed kernel extracts of *A. hippocastanum* obtained by SE was constituted manly the *O*-glycosylated quercetin, kaempferol, and isorhamnetin derivatives (representing ≥ 90 %), but caffeic acid and catechin derivatives were also present. The four aescin saponins, namely aescin Ia, aescin Ib, isoaescin Ia, and isoaescin Ib, were also detected. The SE of these seed phytoconstituents was successfully modelled by accurately fitting the quantitative data to a second-order polynomial equation, which allowed accessing linear, quadratic and interaction effects of the factors *t*, *P* and *S* on the target responses. The ethanol proportion stood out as the most critical factor and was the main responsible for the selectivity of the SE processes. In general, it was possible to recover the main *A. hippocastanum* seed compounds using short processing times, medium-low ultrasonic powers, and high ethanol proportions, representing a technological advance compared to methods available for industrial exploitation. The obtained flavonol/aescin-rich extracts could be used by pharmaceutical, cosmetic, and food industries, and the inherent production processes adopted by biorefineries. Future studies will be of interest to evaluated the biological activities of the different extracts obtained in this work.

CRediT authorship contribution statement

Maria Inês Dias: Methodology, Validation, Formal analysis, Investigation, Writing – original draft, Writing – review & editing, Supervision. **Carly Albiston:** Methodology, Validation, Formal analysis, Investigation, Writing – original draft. **Mikel Añibarro-Ortega:** Formal analysis, Investigation. **Isabel C.F.R. Ferreira:** Conceptualization, Writing – review & editing. **José Pinela:** Conceptualization, Methodology, Validation, Formal analysis, Writing – original draft, Writing –

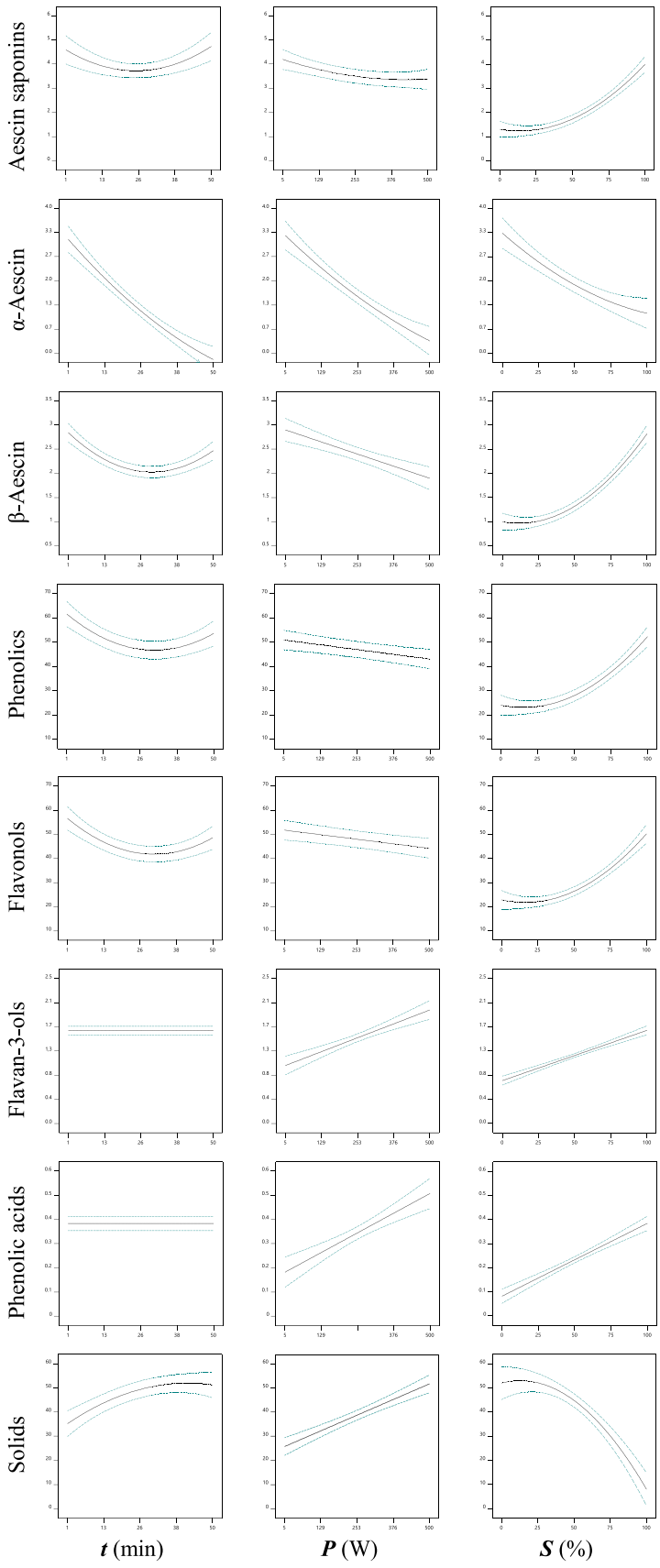

Fig. 5. Response plots for the effects of each factor (*t*: time, *P*: power, and *S*: ethanol proportion) on the extraction of solids (Y_1) and groups of compounds (Y_2–Y_8) from horse chestnut seed kernel. In each 2D plot, the omitted factors were set at their individual optimum in Table 5.

review & editing, Supervision, Supervision. **Lillian Barros:** Conceptualization, Validation, Resources, Writing – review & editing, Supervision.

Declaration of Competing Interest

The authors declare that they have no known competing financial interests or personal relationships that could have appeared to influence the work reported in this paper.

Acknowledgments

The authors are grateful to the Foundation for Science and Technology (Fundação para a Ciência e a Tecnologia (FCT), Portugal) for financial support by national funds FCT/MCTES to CIMO (UIDB/00690/2020); to FCT for the PhD studentship granted to M. Añibarro-Ortega (2020.06297. BD) and the contracts of M.I. Dias and L. Barros (institutional scientific employment program-contract) and J. Pinela (CEECIND/01011/2018). To the European Regional Development Fund (FEDER) through the Regional Operational Program North 2020, within the scope of the Project GreenHealth - Norte-01–0145-FEDER-000042.

Appendix A. Supporting information

Supplementary data associated with this article can be found in the online version at doi:10.1016/j.indcrop.2022.115142.

References

Abudayeh, Z.H.M., al Azzam, K.M., Naddaf, A., Karpiuk, U.V., Kislichenko, V.S., 2015. Determination of four major saponins in skin and endosperm of seeds of horse chestnut (*Aesculus hippocastanum* L.) using high performance liquid chromatography with positive confirmation by thin layer chromatography. Adv. Pharm. Bull. 5, 587–591. https://doi.org/10.15171/APB.2015.079.

Alara, O.R., Abdurahman, N.H., Ukaegbu, C.I., 2021. Extraction of phenolic compounds: a review. Curr. Res. Nutr. Food Sci. 4, 200–214. https://doi.org/10.1016/J.CRFS.2021.03.011.

Amiri, S., Shakeri, A., Sohrabi, M.R., Khalajzadeh, S., Ghasemi, E., 2019. Optimization of ultrasonic assisted extraction of fatty acids from *Aesculus hippocastanum* fruit by response surface methodology. Food Chem. 271, 762–766. https://doi.org/10.1016/J.FOODCHEM.2018.07.144.

Aronson, J.K., 2016. Hippocastanaceae. In: Meyler's Side Effects of Drugs: The International Encyclopedia of Adverse Drug Reactions and Interactions. Elsevier, p. 750. https://doi.org/10.1016/B978-0-444-53717-1.00848-9.

Barros, L., Calhelha, R.C., Queiroz, M.J.R.P., Santos-Buelga, C., Santos, E.A., Regis, W.C. B., Ferreira, I.C.F.R., 2015. The powerful *in vitro* bioactivity of *Euterpe oleracea* Mart. seeds and related phenolic compounds. Ind. Crops Prod. 76, 318–322. https://doi.org/10.1016/J.INDCROP.2015.05.086.

Bessada, S.M.F., Barreira, J.C.M., Barros, L., Ferreira, I.C.F.R., Oliveira, M.B.P.P., 2016. Phenolic profile and antioxidant activity of *Coleostephus myconis* (L.) Rchb.f.: an underexploited and highly disseminated species. Ind. Crops Prod. 89, 45–51. https://doi.org/10.1016/j.indcrop.2016.04.065.

Caleja, C., Barros, L., Prieto, M.A., Barreiro, M.F., Oliveira, M.B.P.P., Ferreira, I.C.F.R., 2017. Extraction of rosmarinic acid from *Melissa officinalis* L. by heat-, microwave- and ultrasound-assisted extraction techniques: a comparative study through response surface analysis. Sep. Purif. Technol. 186, 297–308. https://doi.org/10.1016/j.seppur.2017.06.029.

Chemat, F., Rombaut, N., Sicaire, A.G., Meullemiestre, A., Fabiano-Tixier, A.S., Abert-Vian, M., 2017. Ultrasound assisted extraction of food and natural products. Mechanisms, techniques, combinations, protocols and applications. A review. Ultrason. Sonochem. 34, 540–560. https://doi.org/10.1016/J.ULTSONCH.2016.06.035.

Chen, J., Li, W., Yang, B., Guo, X., Lee, F.S.C., Wang, X., 2007. Determination of four major saponins in the seeds of *Aesculus chinensis* Bunge using accelerated solvent extraction followed by high-performance liquid chromatography and electrospray-time of flight mass spectrometry. Anal. Chim. Acta 596, 273–280. https://doi.org/10.1016/J.ACA.2007.06.011.

Cheok, C.Y., Salman, H.A.K., Sulaiman, R., 2014. Extraction and quantification of saponins: a review. Food Res. Int. 59, 16–40. https://doi.org/10.1016/J.FOODRES.2014.01.057.

Cheong, D.H.J., Arfuso, F., Sethi, G., Wang, L., Hui, K.M., Kumar, A.P., Tran, T., 2018. Molecular targets and anti-cancer potential of escin. Cancer Lett. 422, 1–8. https://doi.org/10.1016/J.CANLET.2018.02.027.

Čukanović, J., Tešević, V., Jadranin, M., Ljubojević, M., Mladenović, E., Kostić, S., 2020. Horse chestnut (*Aesculus hippocastanum* L.) seed fatty acids, flavonoids and heavy metals plasticity to different urban environments. Biochem. Syst. Ecol. 89, 103980 https://doi.org/10.1016/J.BSE.2019.103980.

Dridi, A., 2018. Chemical composition and bioactivity of different botanical parts of *Aesculus hippocastanum* L. fruits. Master dissertation in Chemical Engineering. Instituto Politécnico de Bragança, Portugal, and Tunisia Private University ULT, Tunisia.

EMA, European Medicines Agency, 2008. European Union herbal monograph on *Aesculus hippocastanum* L., semen. Final-Revision 1. EMA/HMPC/628242/2018. Amsterdam, The Netherlands.

EMA, European Medicines Agency, 2020. Assessment report on *Aesculus hippocastanum* L., semen. EMA/HMPC/638244/2018. Amsterdam, The Netherlands.

Gagić, T., Knez, Ž., Škerget, M., 2021. Subcritical water extraction of horse chestnut (*Aesculus hippocastanum*) tree parts. J. Serbian Chem. Soc. 86, 603–613. https://doi.org/10.2298/JSC201111013G.

Giordano, M., Pinela, J., Dias, M.I., Calhelha, R.C., Stojković, D., Soković, M., Tavares, D., Cánepa, A.L., Ferreira, I.C.F.R., Caleja, C., Barros, L., 2021. Ultrasound-assisted extraction of flavonoids from kiwi peel: process optimization and bioactivity assessment. Appl. Sci. 11 https://doi.org/10.3390/APP11146416.

Horvath, E.Dr., 1991. Method for the production of extracts rich in beta-aescin. EP0298148B1.

Hübner, G., Wray, V., Nahrstedt, A., 1999. Flavonol oligosaccharides from the seeds of *Aesculus hippocastanum*. Planta Med. 65, 636–642. https://doi.org/10.1055/S-1999-14038.

Iberahim, N., Sethupathi, S., Goh, C.L., Bashir, M.J.K., Ahmad, W., 2019. Optimization of activated palm oil sludge biochar preparation for sulphur dioxide adsorption. J. Environ. Manage. 248, 109302 https://doi.org/10.1016/j.jenvman.2019.109302.

Jiang, N., Xin, W., Wang, T., Zhang, L., Fan, H., Du, Y., Li, C., Fu, F., 2011. Protective effect of aescin from the seeds of *Aesculus hippocastanum* on liver injury induced by endotoxin in mice. Phytomedicine 18, 1276–1284. https://doi.org/10.1016/J.PHYMED.2011.06.011.

Kameyama, A., Fujimura, T., 2016. Method for producing Hippocastanaceae plant seed extract. US20100310689A1.

Kapusta, I., Janda, B., Szajwaj, B., Stochmal, A., Piacente, S., Pizza, C., Franceschi, F., Franz, C., Oleszek, W., 2007. Flavonoids in horse chestnut (*Aesculus hippocastanum*) seeds and powdered waste water byproducts. J. Agric. Food Chem. 55, 8485–8490. https://doi.org/10.1021/JF071709T.

Kochan, E., Szymańska, G., Wielanek, M., Wiktorowska-Owczarek, A., Jóźwiak-Bębenista, M., Grzegorczyk-Karolak, I., 2019. The content of triterpene saponins and phenolic compounds in American ginseng hairy root extracts and their antioxidant and cytotoxic properties. Plant Cell Tissue Organ Cult. 138, 353–362. https://doi.org/10.1007/S11240-019-01633-3/FIGURES/1.

Küçükkurt, I., Ince, S., Keleş, H., Küpeli Akkol, E., Avci, G., Yeşilada, E., Bacak, E., 2010. Beneficial effects of *Aesculus hippocastanum* L. seed extract on the body's own antioxidant defense system on subacute administration. J. Ethnopharmacol. 129, 18–22. https://doi.org/10.1016/J.JEP.2010.02.017.

Kurt, D., 1965. Method of producing durable saponin containing extracts from horse chestnut and products obtained therefrom. US3170916A.

Liao, Y., Li, Z., Zhou, Q., Sheng, M., Qu, Q., Shi, Y., Yang, J., Lv, L., Dai, X., Shi, X., 2021. Saponin surfactants used in drug delivery systems: a new application for natural medicine components. Int. J. Pharm. 603, 120709 https://doi.org/10.1016/J.IJPHARM.2021.120709.

Lin, L.Z., Chen, P., Ozcan, M., Harnly, J.M., 2008. Chromatographic profiles and identification of new phenolic components of *Ginkgo biloba* leaves and selected products. J. Agric. Food Chem. 56, 6671. https://doi.org/10.1021/JF800488X.

Matsuda, H., Li, Y., Murakami, T., Ninomiya, K., Araki, N., Yoshikawa, M., Yamahara, J., 1997. Antiinflammatory effects of escins Ia, Ib, IIa, and IIb from horse chestnut, the seeds of *Aesculus hippocastanum* L. Bioorg. Med. Chem. Lett. 7, 1611–1616. https://doi.org/10.1016/S0960-894X(97)00275-8.

Melgar, B., Pereira, E., Oliveira, M.B.P.P., Garcia-Castello, E.M., Rodriguez-Lopez, A.D., Sokovic, M., Barros, L., Ferreira, I.C.F.R., 2017. Extensive profiling of three varieties of *Opuntia* spp. fruit for innovative food ingredients. Food Res. Int. 101, 259–265. https://doi.org/10.1016/J.FOODRES.2017.09.024.

Meullemiestre, A., Breil, C., Abert-Vian, M., Chemat, F., 2016. Microwave, ultrasound, thermal treatments, and bead milling as intensification techniques for extraction of lipids from oleaginous *Yarrowia lipolytica* yeast for a biojetfuel application. Bioresour. Technol. 211, 190–199. https://doi.org/10.1016/J.BIORTECH.2016.03.040.

Mitscher, L.A., 2007. Traditional medicines. Comprehensive Medicinal Chemistry II. Elsevier, pp. 405–430. https://doi.org/10.1016/B0-08-045044-X/00012-2.

Pinela, J., Prieto, M.A., Barros, L., Carvalho, A.M., Oliveira, M.B.P.P., Saraiva, J.A., Ferreira, I.C.F.R., 2018. Cold extraction of phenolic compounds from watercress by high hydrostatic pressure: Process modelling and optimization. Sep. Purif. Technol. 192, 501–512. https://doi.org/10.1016/j.seppur.2017.10.007.

Rocha, R., Pinela, J., Abreu, R.M.V., Añibarro-Ortega, M., Pires, T.C.S.P., Saldanha, A.L., Alves, M.J., Nogueira, A., Ferreira, I.C.F.R., Barros, L., 2020. Extraction of anthocyanins from red raspberry for natural food colorants development: Processes optimization and in vitro bioactivity. Processes 8, 1447. https://doi.org/10.3390/pr8111447.

Silva, A.R., Pinela, J., García, P.A., Ferreira, I.C.F.R., Barros, L., 2021. *Cytinus hypocistis* (L.) L.: optimised heat/ultrasound-assisted extraction of tannins by response surface methodology. Sep. Purif. Technol. 276, 119358 https://doi.org/10.1016/J.SEPPUR.2021.119358.

Singh, B., 2006. A simple process for obtaining beta-aescin from Indian horse chestnut (*Aesculus indica*). EP1487847B1.

Sirtori, C.R., 2001. Aescin: pharmacology, pharmacokinetics and therapeutic profile. Pharmacol. Res. 44, 183–193. https://doi.org/10.1006/PHRS.2001.0847.

Vujic, Z., Novovic, D., Arsic, I., Antic, D., 2013. Optimization of extraction process of escin from dried seeds of *Aesculus hippocastanum* L. by Derringer's desirability function. J. Anim. Plant Sci. 17, 2514–2521.

Xiao, Z., He, L., Hou, X., Wei, J., Ma, X., Gao, Z., Yuan, Y., Xiao, J., Li, P., Yue, T., 2021. Relationships between structure and antioxidant capacity and activity of glycosylated flavonols. Foods 10, 849. https://doi.org/10.3390/FOODS10040849/S1.

Zhang, Z., Li, S., Lian, X.-Y., 2014. An Overview of genus *Aesculus* L.: ethnobotany, phytochemistry, and pharmacological activities. Pharm. Crop 1, 24–51. https://doi.org/10.2174/2210290601001010024.

Zhao, S.Q., Xu, S.Q., Cheng, J., Cao, X.L., Zhang, Y., Zhou, W.P., Huang, Y.J., Wang, J., Hu, X.M., 2018. Anti-inflammatory effect of external use of escin on cutaneous inflammation: possible involvement of glucocorticoids receptor. Chin. J. Nat. Med. 16, 105–112. https://doi.org/10.1016/S1875-5364(18)30036-0.

Zhao, W., Lao, Y., Liu, Y., Niu, J., Xiao, Z., Arulselvan, P., Shen, J., 2022. Escin induces apoptosis in ovarian cancer cell line by triggering S-phase cell cycle arrest and p38 MAPK/ERK pathway inhibition. J. King Saud Univ. Sci. 34, 101644 https://doi.org/10.1016/J.JKSUS.2021.101644.